Journal of Engineering and Science Research 6 (1): 10-17, 2022
e-ISSN: 2289-7127

DOI: 10.26666/rmp.jesr.2022.1.2

Geophysical Analysis on Electrical Resistivity Technique Toward Composite of Geostrata

Noorasyikin,M.N[1] and Zainab,M[2]
Universiti Tun Hussein Onn Malaysia[1], Universiti Teknologi Mara[2]
Batu Pahat,Johor[1],Shah Alam,Selangor[2] Malaysia

Abstract: Primarily geophysical techniques are the most widely used method that considers the safety, cost, and time-saving aspects. There are several techniques of geophysical techniques such as electrical resistivity, seismic, magnetic and ground penetrating radar. Among of the geophysical techniques, electrical resistivity is the best technique to detect subsurface abnormalities such as mine void; fractures, water level, and it can also identify the types of materials as either soil or rock. In this study, a laboratory model study of tank was carried out with different layers of geostrata. A forty-one of 15cm copper electrodes were set up in the tank at 0.04 meter spacing and Wenner protocol was applied. The main objectives of this study are to determine the 2D georesistivity profiling of stratified soil and hard layers. Based on observation, it was found that the georesistivity of materials were depending on several parameters such as moisture content, porosity and mineralogy.

Key words: *2D Electrical Resistivity, geomaterials, Wenner protocol, tank modeling, mineralogy*

INTRODUCTION

Electrical Resistivity technique is a measure of how the current ability passes through the ground materials [2]. In this study, the word georesistivity is introduced to name the electrical resistivity of geomaterial. The main purpose of georesistivity survey is to determine the subsurface of the ground structure by making a measurement at the surface with the resistivity equipment [4]. Georesistivity of the material is measured by injecting the current into the ground [3]-[5] with electrodes which are connected to the ABEM Terrameter SAS 4000 System and Electrode Selector. The flow of current from one electrode to another electrode will measure the datum point in the subsurface of the ground [4]. This datum point is called pseudosection. This pseudosection was calculated and inverted by using RES2DINV software [4]-[1] to produce subsurface images with detailed georesistivity index which are represented in color contours.

EXPERIMENT

Materials And Methods

A. Soil classification and Particle Density of Geomaterials

The grain size was analyzed by applied dry sieve analysis test to classify the soil. The apparatus that were used to conduct the test were sieves with different aperture sizes, a weighing balance, a sample divider (riffle box), an oven, a sieve brusher and a mechanical sieve shaker. Before start the experiment, the sieve size was firstly cleaned using the sieve brushes. The procedure of this test was carried out based on BS 1377: Part 2: 1990: Clause 9.2.2. Figure 1 shows the soil was put into the sieve shaker to sieve the soil. After finish the test, the graph was plotted by using the Particle Size Distribution software.

The particle density of soil was conducted to determine the porosity of soil. The test was carried out based on BS 1377-2:1990. The apparatus that was used for this test are cylinder measurement and tap water.

Corresponding Author: Noorasyikin Bt Mohammad Noh, Universiti Tun Hussein Onn Malaysia, Malaysia, Email: shecan83us@gmail.com

B. Soil Mineralogy and Petrographic study

To determine composition of mineralogy in soil sample, X-Ray Diffraction Test was implemented. To carry out this test, the soil sample had to be in powder form and dried in the oven for about 24 hours at temperature 300^0 C., The soil sample was sieved at 0.15 mm size by using the sieve shaker to get the sample in powder form. The apparatus that were applied for this test are an x-ray diffractometer, a glass sample plate, a spatula, a glove, and a balance. The procedure of this test was carried out based on ASTM 2369 Standard Method. The glass sample plate with soil sample was placed at the sample holder in the x-ray diffractometer machine. The mineralogy of soil was obtained by analyzing the soil at 2-90 degrees by default under crossed polarized light using the x-ray diffractometer machine.

The study of minerals and textures of hard material by thin section is called as petrography study. Cement mortar samples were tested to get the unknown minerals composite in the sample. Thin section petrography is the study of microscopic features using a "polarizing" or "petrographic" microscope. A thin section was made from it to look at a sample through a microscope. Thin sections were made from small slabs of a cement mortar sample glued to a glass slide (~1 inch by 2 inches), and then ground to a specified thickness of 0.03 mm (30 microns). At this thickness most minerals become more or less transparent and can then be analyzed by a microscope using transmitted light. The procedure of the test was carried out based on the International Society for Rock Mechanics (ISRM- Year 1974 - 2006) Suggested Method. The apparatus that were used to conduct this experiment were a thin section discoplan, a double wheel grinder, a petrographic microscope, a polisher, carborundum, grease, a sample container, a disposable container, acetone, Canada balsam, xylene A & B, a hot plate, a vacuum impregnation machine and army acetate.

C.Tank Modeling – 2D Resistivity Profiling

A laboratory model study was carried out by constructing a tank filled with composite of geostrata. The tank was modelled to derive the images of the stratified geomaterials. The size of tank was 183cm in length, 39cm in width, and 100cm in height and filled up with density of geomaterials $2g/cm^3$.Forty-one copper electrodes at 15cm in length were used and installed at 0.04 meter spacing in the tank.

In this study, the geostrata was modelled as Model 1, Model 2, Model 3, and Model 4. These models were connected to the ABEM Terrameter SAS4000 and ABEM electrode selector to conduct the resistivity test. The protocol that was used in this study was the Wenner array. This protocol was used because it has strong signal strength whereby the data will not be affected by loud noises. Besides that, this Wenner-Short protocol was also suitable because the test was conducted in the tank with limited length of about 183cm. From the georesistivity survey, the datum point was collected. This datum point is called pseudosection. This pseudosection was calculated and inverted by using RES2DINV software to produce subsurface image with detailed georesistivity index which represented in color contours. Figure 1, Figure 2, Figure 3 and Figure 4 shows the schematic layout of tank with stratified materials.

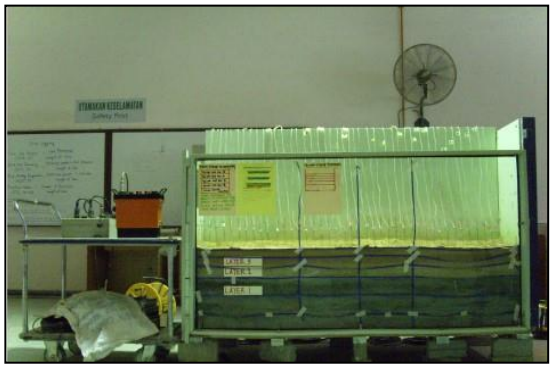

Figure 1: Model 1 (Dry condition) and Model 2 (0.5%, 5.0%, and 10.0%) by weight of water

Figure 2: Model 2 with Soil Moisture Probe – Undrained condition

Figure 3: Model 3 with Soil Moisture Probe – Undrained and Drained condition

Figure 4: Model 4 with surcharge load

RESULTS & ANALYSIS

A.Soil classification and Particle Density of Geomaterials

The soil particle size distributions are classified as shown in Table1. Based on the results, it was found that the name of the soil was well-graded sand in which was based on the highest percentage of sand particles ranging between 60% to 80%. These soils also met the criteria of the British Soil Standard where the soil samples had a coefficient of uniformity (C_U) value above 6.0 and coefficient of gradation (Cg) value between 1 and 3. If both of these criteria are met, the sand is classified as well-graded or SW. For the porosity of soil, it is shows that the porous of hard layer consist 26% while the sandy soil obtained 19%.

Table 1: Particle Size Distribution of Sedimentary Residual soils

Table 1: Particle Size Distribution of Sedimentary Residual soils

Sample	Soil Types	% Gravel	% Sand	%Fine
Soil layer 1	Well-graded sand	27.24	69.70	3.05
Soil layer 2	Well-graded sand	30.83	68.81	0.37
Soil layer 3	Well-graded sand	21.14	77.21	1.65

B.Soil Mineralogy and Petrographic study

Figure 5 shows the plot of Intensity versus 2-Theta degrees. The 2-Theta degrees represented the degree of crossed light during the soil analysis using the X-Ray Diffractometer. The intensity represents the soil mineralogy that was detected under diffraction light. Table 2 shows different classes of minerals obtained. From the results obtained, it shows that the soil contains high clay mineralogy. The clay mineral is known to absorb and sustain water easily. The clay minerals tend to ionize and contribute to the supply of free ions. From these two characteristics, clay mineralogy therefore has low resistivity or high conductivity as compared to the rest of the minerals.

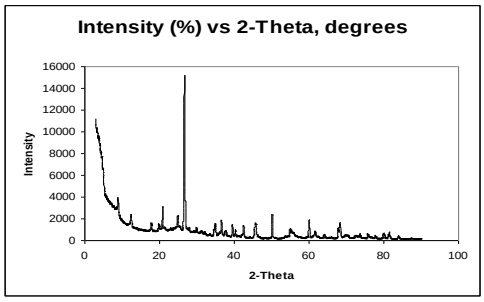

Figure 5: Graph Intensity versus 2-Theta Degrees

Table 2: Classes of Soil Minerals

Classes of Minerals	Number of Minerals
Clay	23
Silicates	11
Phosphates	5
Borates	3
Vanadate	0
Nitride	0
Sulfide	6
Carbonates	0
Oxides	0

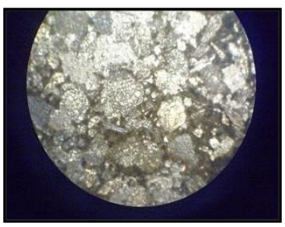

Figure 6: Micro texture of cement mortar

Figure 6 shows the cemented texture of the cement mortar constituted of silica sand grains with Portland cement also known as calcite as the filler under 4x microscope. The monochrome color of the silica sand in black, grey and off-white indicated the reflection and refraction of light on the silica sand particles of size 0.05 mm diameter.

C. Tank Modeling – 2D Resistivity Profiling

Model 1 – Dry Condition

This model was carried out in dry condition with cement mortar (as bedrock) and sandy soil (layer 1 and layer 2) in the tank respectively. Since the soil strata were relatively oven-dried samples, no output was obtained as all 41 electrodes could not give any reading of soil mass conductivity.

Model 2 - Geostrata at Wet Undrained Condition

This model was carried out in wet and undrained condition with cement mortar (as bedrock) and sandy soil (layer 1 and layer 2) in the tank respectively. Figure 7 shows the image of geostrata for Model 2 by 0.5% weight of water. The image presents in homogeneous layer similar to actual condition. The RMS error was found to be 29.1% where it is acceptable for interpretation where produce good reliable image. The georesistivity images reading was repeated when Model 2 was wetted at 5.0% and 10% and subsequently the results were analyzed in the same manner. It was noted that at 5.0% and 10.0% by weight of water the RMS errors were 19.8% and 9.9% respectively, below 30.0% as the control. Figure 5 shows the georesistivity analysis for Model 2 in wet condition by different weight of water (0.5%, 5.0% and 10%).

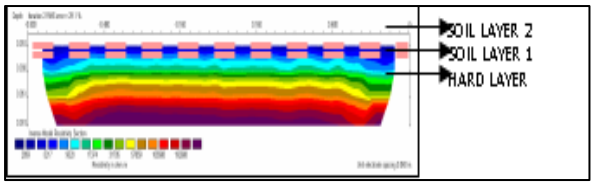

Figure 7: Georesistivity images for Model 2 at 0.5% by weight of water

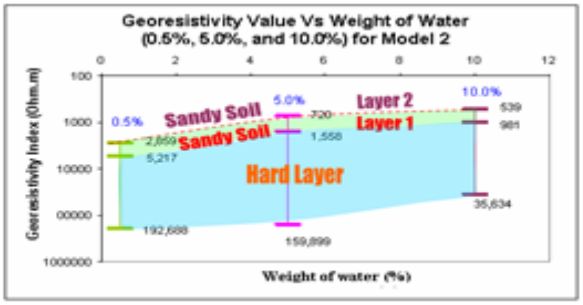

Figure 8: Graph georesistivity value versus weight of water (0.5%, 5.0% and10.0%) for Model 2

From Figure 8, at 0.5% by weight of water, sandy soil layer 2 and sandy soil layer 1 had georesistivity value ranging from 2,859 Ωm to 5,217 Ωm. Meanwhile, at 5.0% by weight of water, the georesistivity value decreased by 74.8% with range values from 720 Ωm to 1,558 Ωm**.** At 10.0% by weight of water, the georesistivity value also decreased by 25.1% with range values from 539 Ωm to 981 Ωm, differed by 442 Ωm .The clay mineralogy contains in the soil sample affect to the soil samples by ionizing and supplied free ions.

For hard layer, at 0.5% by weight of water, the range of georesistivity value was wider as compared to 5.0% and10.0% which ranged from 5,217 Ωm to 192,688 Ωm. This could be due to less presence of free ions from the water molecules Hence, because of less weight of water, the hard layer acquired high values of georesistivity at 0.5% by weight of water. In addition, the silicate mineralogy contains in hard layer gave affect which lead to high resistivity values. On the other hand, at 5.0% by weight of water, the georesistivity values decreased by 17.0% which ranged from 1,558 Ωm to 159,899 Ωm. Nevertheless, at 10.0% by weight of water, the hard layer had the greatest percentage of decreases in georesistivity values of about 77.7%, ranging from 981 Ωm to 35,634 Ωm. Due to the large pore space of 26.0% in the hard layer, this porosity influenced the water to be filled up between the pore spaces of hard layer. Hence, because of this reason, the hard layer consisted of low georesistivity value. In summary, the increases in moisture content influenced the changes of georesistivity value where it gave very low value depending on the porosity of the geomaterials. Hence, it can be summarized that although the density for each layer of geomaterials is the same, the porosity and

moisture content of the materials may influence the georesistivity value.

Model 2 - Geostrata at Undrained Condition

For Model 2 in undrained condition, the geomaterials were allowed to be air-dried. It was observed that the georesistivity value and moisture content of the geomaterials changed from Day 1 to Day 7. The trend lines of sandy soil layer 2 and sandy soil layer 1 are parallel. At Day 1, the georesistivity value for sandy soil layer 2, sandy soil layer 1 and hard layer was relatively lower with maximum value of 141 Ωm, 159 Ωm and 330 Ωm respectively at 15.55% moisture reading. At undrained condition, the hard layer, instead of showing higher resistivity that sandy soils above but due to the self-draining properties of sandy soil, the moisture has saturate the hard layer mass, giving resistivity value of 330 Ωm. The soil moisture probe reading showed evidence that hard layer had moisture content of 15.55%. At the end of Day 7, the values for sandy soil layer 2, sandy soil layer 1 and hard layer increased slightly where the differences for soil layer 2 was 90 Ωm, in which was equivalent to 39% . Soil layer 1 had difference of 86 Ωm, equivalent to 35% and for hard layer it was only 4.62 % at difference in moisture of 4.16% for all materials. The findings show that residual soil with some clay content is very sensitive to slight change in moisture as compared to cement mortar.

Model 3 – Undrained and Drained Condition

Model 3 is where Model 2 composite strata was topped up with another layer of sandy soil represent as sandy soil layer 3 and finally capped with another hard layer as shown in Figure 1. Model 3 was filled and flooded with tap water from the top surface and left to self-dry at room temperature for 24 hours. The georesistivity readings were then taken. The thickness of each geomaterials strata was measured from the georesistivity image as shown in Figure 9 at undrained condition. The thickness of georesistivity image for top hard layer was calculated to be 13.06 mm. Sandy soil layer 3, sandy soil layer 2, sandy soil layer 1 and bottom hard layer were calculated to be 26.10 mm, 4.35 mm, 4.35 mm and 26.1 mm respectively, totaling up to 74.00 mm of image for 850 mm total thickness of geomaterials.

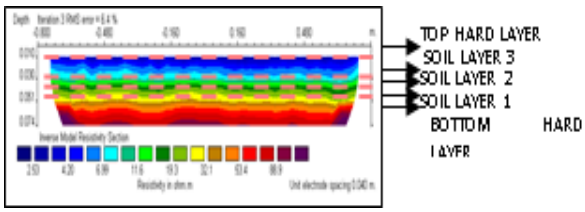

Figure 9: Model 3 in undrained condition for Day 1

The different color codes represent the strata of geomaterials Model 3 at moisture reading of 29.91% (top hard layer) and 40.76% for soil layer 3 to soil layer 1. The dark blue layer represents hard layer at top where the georesistivity value is 2.53 Ωm. For blue, custom blue, light blue, custom light blue, turquoise, and custom light green colors, these layer colors represent sandy soil layer 3. The georesistivity value for sandy soil layer 3 ranged from 4.20 Ωm to 11.6 Ωm. For sandy soil layer 2, the georesistivity value ranged from 11.6 Ωm to 19.3 Ωm in which is represented by bright green and green colors in the table. Meanwhile, the georesistivity value for sandy soil layer 1 ranged from 19.3 Ωm to 32.1 Ωm, in which is represented by lime and yellow colors. It was observed that the flow of ion electricity in the sandy soil layer 3 was more conductive than in sandy soil layer 1. This was because sandy soil layer 3 was at the uppermost surface and at the shortest travel distance to the source of current transmit via the soil mass as compared to sandy soil 1 and sandy soil layer 2.

Figure 10 shows the graph of comparative georesistivity index for hard layer represented by Model 2 and Model 3 both at undrained condition for Day 1 to Day 7. The objective was to determine the characteristics of the georesistivity image of the hard layer when it is at the top as compared at the bottom of the tank. It was noted that the georesistivity value of hard layer for Model 3 ranged from 2.53 Ωm (Day 1) to 3.68 Ωm (Day 7) with recorded moisture ranged from 29.91% (Day 1) to 25.1% (Day 7). Meanwhile, for Model 2, the georesistivity value of hard layer ranged from 330 Ωm (Day 1) to 346 Ωm (Day 7) with recorded moisture that ranged from 15.55% (Day 1) to11.39% (Day 7). Results showed that although the hard layer had the same properties, but the moisture content had significantly determined the georesistivity value of the hard layer besides its mineral compositions. Figure 11 shows the graph of comparative georesistivity index for sandy soil layer 1 and sandy soil layer 2 represented by Model 2

and Model 3 both at undrained condition for Day 1 to Day 7.

The objective was to determine the characteristics of the georesistivity image of sandy soils between two Models. The Figure shows the trend of georesistivity value for sandy soil layer 1 and sandy soil layer 2 that represent each Model; Model 2 and Model 3 in undrained condition.

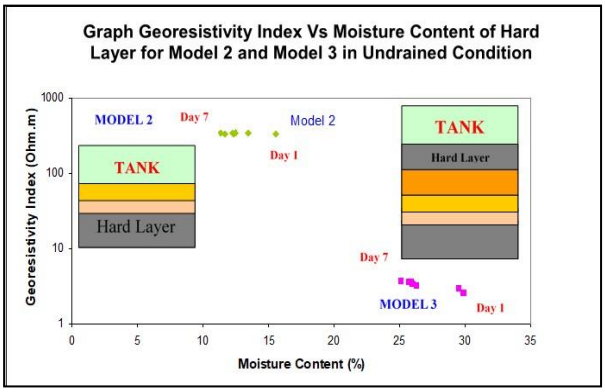

Figure 10: Graph of georesistivity index versus moisture content of hard layer for Model 2 and Model 3 in undrained condition

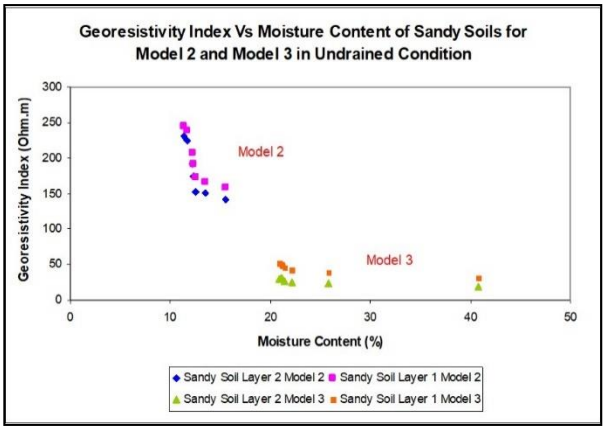

Figure 11: Graph of georesistivity index versus moisture content of sandy soils for Model 2 and Model 3 in undrained condition

The blue and pink marks represent sandy soil layer 2 and sandy soil layer 1 respectively for Model 2 at undrained condition. Meanwhile, green and orange colors represent sandy soil layer 2 and sandy soil layer 1 for Model 3, which was also at undrained condition. In Model 2, the georesistivity value for both sandy soils ranged from 141 Ωm (Day 1) to 245 Ωm (Day 7) with recorded moisture that ranged from 15.55% (Day 1) to 11.39% (Day 7), in which reduced by 26.8%. However, in Model 3 the georesistivity value presented low value which ranged from 11.6 Ωm (Day 1) to 51.3 Ωm (Day 7) with recorded moisture that ranged from 40.76% (Day 1) to 20.92% (Day 7). Comparatively, the georesistivity values for Model 2 and Model 3, differed in total by 79.0%. An additional soil layer 3 capped by hard layer and saturated for 1 day that made up Model 3 made the degree of moisture in Model 3 higher than Model 2. Soil moisture probe reading indicated that Model 2 had range of moisture from 11.39% to 15.55% while Model 3 had moisture content of 20.92% to as high as 40.76%. Hence, this was justified by the georesistivity images observed for both models.

Model 4 – Effect of Surcharge Load

After one month observation, Model 3 was uniformly loaded with concrete cubes at three different surcharge loads of 0.7 kN/m, 1.0 kN/m and 2.0 kN/m for 24 hours each. A comparative analysis of the overall georesistivity images with surcharge load (Model 4) and without surcharge load (Model 3) was carried out as shown in Figure 9 below. As the soil layers were more compressible than hard layer, it could be seen that at 0.7 kN/m surcharge, Model 4 lateral color images distorted vertically as compared to Model 3 color images. The lateral colour images are more uniform without surcharge as compared to with surcharge. The differences in the georesistivity value due to the surcharge that caused the densification of compressible soil are plotted as shown in Figure 12.

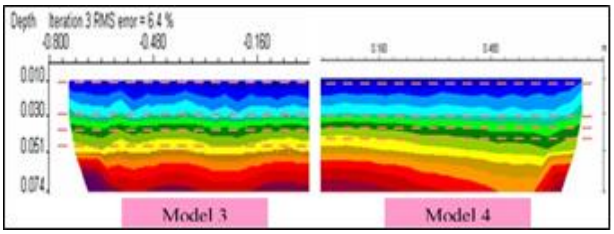

Figure 12: Comparison of georesistivity image without surcharge (Model 3) and with surcharge load of 0.7 kN/m (Model 4)

Without surcharge, the georesistivity of compressible soil layers were 9.48 Ωm for layer 3, 28.5 Ωm for layer 2 and 49.4 Ωm for layer 1. At surcharge load 0.7 kN/m, the georesistivity value of sandy soil layer 3, sandy soil layer 2 and sandy soil layer 1 were 17.3 Ωm, 30.1 Ωm, and 52.2 Ωm respectively with recorded moisture of 19.92%. It was noted that the georesistivity value increased from Model 3 result at Week 4. At surcharge load of 2.0kN/m, the georesistivity value of sandy soil layer 3 had difference of 1.8 Ωm, equivalent to 10.4%. Moreover, sandy soil layer 2 had difference of 1.6 Ωm, equivalent to 5.3% while sandy soil layer 1 had difference of 0.6 Ωm at recorded moisture of 19.62%. The % of moisture content reduced by 0.91% at surcharge load 2.0 kN/m.

It was observed that as the surcharge load increased, the georesistivity value of sandy soils increased slightly due to its compressible effect. The total percentage difference was 50.4%. This was because as the compressible soil densified the pore volume, the moisture was expelled. Thus, naturally, the georesistivity increases were well-represented by the georesistivity image. Figure 13 shows the graph of georesistivity value versus moisture content for sandy soils at three different surcharge loads (0.7KN/m, 1.0KN/m, and 2.0KN/m).

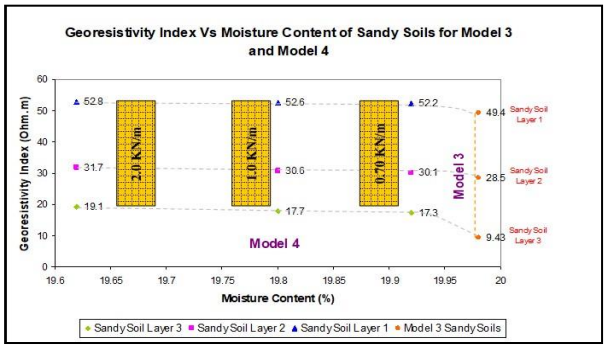

Figure 13: Graph of georesistivity index versus moisture content for Model 4 (soil layers) at three different surcharge loads

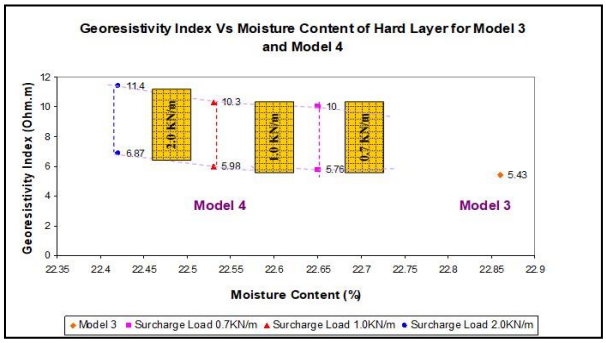

Figure 14: Graph georesistivity index versus moisture content of top hard layer for Model 4 at three surcharge loads

Without surcharge, the top hard layer georesistivity value was less than 5.43 Ωm at 22.86% moisture reading. At surcharge load of 0.7kN/m, the georesistivity value increased to 5.76 Ωm to 10.0 Ωm at recorded moisture of 22.65%. As surcharge load increased to 1.0KN/m and 2.0KN/m, the georesistivity value increased respectively where it ranged from 6.87 Ωm to 11.4 Ωm with recorded moisture of 22.42% finally. The observation of the georesistivity image was further extended for another 3 consecutive weeks where Model 4 was allowed to dry up at a final surcharge load 2.0 kN/m.

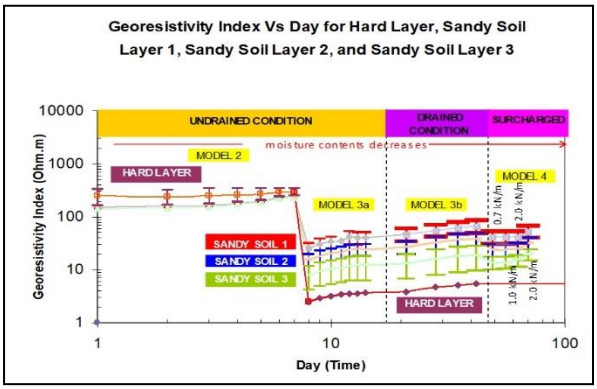

Figure 15: Trend of graph of georesistivity index

CONCLUSION

As a summary, the georesistivity index for all Models showed evidence that the georesistivity index is very much dependent on the degree of moisture content in the pore and types of minerals in the geomaterials. This study has shown good findings that are able to assist in better and accurate interpretation of the georesistivity image determined when using the electrical resistivity technique for subsurface investigation in civil engineering work.

ACKNOWLEDGMENTS

This research was funded by Ministry of Science and Innovation/Esccіencefund reference no 06-01-01-SF 0072 is accordingly acknowledge. Thanks also to SEGi University for giving endless support.

REFERENCES

[1] Batayneh, A.T. (2001). Resistivity Imaging for near surface resistivity dyke using two-dimensional DC resistivity techniques. Journal of Applied Geo Geophysics, 25-32. ELSEVIER.

[2] Brent, R.L. (2003). Applications of Electrical Resistivity: A Surface Geophysical Method. Resource Note No 62.

[3] Lindsay, N.M., Laurence, R.B., & Carl, A.M. (2003). Application of Electrical Resistivity imaging to the development of a geological model for a proposed Edmonton Landfill site. Can.Geotech .J.Volume 40, 551-558.

[4] Loke, M.H. (1999). Electrical Imaging Surveys for Environmental and Engineering Studies. A Practical Guide to 2-D and 3-D Surveys. (Copyright 1997, 1999, 2000).

[5] Solenne, G., Krishna. R., Janardhanan, G., Rana, A., & Chris, P. (2006). Electrical Resistivity Tomography Imaging of Leachate Recirculation in Orchard Hills Landfill. Proceedings of the SWANA Conference, Charlotte.

[6] Sultan, S.A., & Santos, F.A.M. (2007). Evaluating Subsurface Structures and Stratigraphic units using 2D electrical and magnetic data at the area north Greater Cairo, Egypt. International Journal of Applied Earth Observation and Geoinformation, 1-12. Retrieved Feb 1, 2008.

[7] Suman, K.M., Rambhatla, G.S., Ashok, K.P., & Param, K.G. (2008). High resolution 2D electrical resistivity tomography to characterize Active Naitwar Bazar Landslide. Research Articles. Current Science, Vol 94, No.7, pp 871-875.

[8] Tan, C.L., Samsudin, A.R. and Hamzah, U. (2004). Determination subsurface contamination at Sungai Besar Landfill Site using 2-D Resistivity. Malaysian-Japan Symposium on Geohazards and Geoenvironmental Engineering 2004.

[9] Technos. (2004). Surface Geophysical Methods. *Technos, Volume 1. Issue 1*

[10] Torleif, D., & Bing, Z. (2004). A numerical comparison of 2D Resistivity Imaging with 10 electrode arrays. Geophysical Prospecting 2004, 52. European Association of Geoscientists and Engineers.

[11] Umar, H., Abdul Rahim, S., Edna Pilis, M., and Siti Zalifah, J. (2002). *Integrated geological investigation of saltwater intrusion: A case study in Kuala Selangor, Malaysia.* Proceedings of the Regional Symposium on Environment and Natural Sources.Vol 1:402-412.

[12] Umar,H and Mohd Azmi, I. (2009). Geoelectrical resistivity and ground penetrating radar techniques in the study of hydrocarbon contaminated soil. Journal Sains Malaysiana.38(3)(2009):305-311

[11] Victor, R., Martin, G., Victor, F., Carlos, S., and Norbetto.P. (2006). Resistivity Survey of the Subsurface Conditions in the Estuary of the Rio Dela Plata. *Journal of Geotechnical and Geoenvironmental Engineering (ASCE)*, 72-79.

[12] Wanfang Zhou, Barry F.Beck and Angela L.Adams, 2002. *Effective electrode array in mapping karst hazards in electrical resistivity tomography*. Original Article. Environmental Geology (2002).

[13] William, D., Abe Lardo, R., Andrew, B., & Doughlas, L. (2004, May). *Electrical Resistance Tomography. Theory and Practice*. Near Surface Geophysics, Vol 2. 438-442.

[14] Zhou, W., Beck, B.F., & Step, J.B. (2000). *Reliability of dipole-dipole electrical resistivity tomography for detecting depth to bedrock in covered karst terraces.* Research Article. Environmental Geology 39(7).

.